REGULAR ARTICLE

blood advances

A functional DC cross talk promotes human ILC homeostasis in humanized mice

Silvia Lopez-Lastra,[1-3] Guillemette Masse-Ranson,[1,2] Oriane Fiquet,[1,2] Sylvie Darche,[1,2] Nicolas Serafini,[1,2] Yan Li,[1,2] Mathilde Dusséaux,[1,2] Helene Strick-Marchand,[1,2] and James P. Di Santo[1,2]

[1]Innate Immunity Unit, Institut Pasteur, Paris, France; [2]INSERM U1223, Paris, France; and [3]Université Paris-Sud (Paris-Saclay), Ecole Doctorale–Structure et Dynamique des Systèmes Vivants n°577, Paris, France

Key Points

- A novel humanized mouse model to study human ILC biology.
- Human DC cross talk with ILCs in vivo.

Humanized mice harboring human hematopoietic systems offer a valuable small-animal model to assess human immune responses to infection, inflammation, and cancer. Human immune system (HIS) mice develop a broad repertoire of antigen receptor bearing B and T cells that can participate in adaptive immune responses after immunization. In contrast, analysis of innate immune components, including innate lymphoid cells (ILCs) and natural killer (NK) cells, is limited in current HIS mouse models, partly because of the poor development of these rare lymphoid subsets. Here we show that novel dendritic cell (DC)–boosted BALB/c *Rag2*$^{-/-}$*Il2rg*$^{-/-}$*Sirpa*^{NOD}*Flk2*$^{-/-}$ (BRGSF) HIS mice harbor abundant NK cells and tissue-resident ILC subsets in lymphoid and nonlymphoid mucosal sites. We find that human NK cells and ILCs are phenotypically and functionally mature and provide evidence that human DC activation in BRGSF-based HIS mice can "cross talk" to human NK cells and ILCs. This novel HIS mouse model should provide the opportunity to study the immunobiology of human NK cell and ILC subsets in vivo in response to various environmental challenges.

Introduction

Transplantation of human hematopoietic stem cells (HSCs) into immunodeficient mice has been used for the last 2 decades to generate human immune system (HIS) mouse models. HIS mice provide a translational bridge connecting fundamental studies to clinical application and have contributed to the better understanding of human immunity and disease pathogenesis.[1,2] Nevertheless, complete reconstitution of all human hematopoietic lineages and homeostatic long-term maintenance of all human immune cell types has not yet been achieved in these models.[3] Much progress has been made to improve overall human lymphoid and myeloid cell engraftment, and to enhance the development of HLA-restricted T- and B-cell responses. In contrast, the in vivo development of human innate lymphoid effectors, including innate lymphoid cells (ILCs), natural killer (NK) T cells, mucosal-associated invariant T cells, and/or γδT cells, in HIS mice remains suboptimal.

ILCs comprise a recently identified family of immune effector cells that share many functional characteristics with CD4$^+$ T helper cells and CD8$^+$ T cytotoxic lymphocytes (CTLs). As such, ILCs have been proposed as innate versions of T helper cells and CTLs. ILCs derive from committed lymphoid precursors present in the fetal liver and adult bone marrow (BM).[4] ILCs are categorized into 3 main groups according to their transcription factor signatures and cytokine secretion patterns.[5] Group 1 ILCs (ILC1s) include TBET$^+$ cells that produce high levels of interferon-γ (IFN-γ). Among ILC1s, 2 subgroups are appreciated for differences in expression of EOMES. NK cells are EOMES$^+$ and represent an

Submitted 3 January 2017; accepted 15 March 2017. DOI 10.1182/bloodadvances.2017004358.

The full-text version of this article contains a data supplement.

extensively studied ILC subset with cytotoxic activity against virus-infected and tumor cells.[6,7] A second ILC1 subset does not express EOMES and lacks cytotoxic granules but expresses the interleukin-7 (IL-7) receptor (CD127). The "noncytotoxic" ILC1s are associated with epithelium in the liver, lung, and intestine.[8] Group 2 ILCs (ILC2s) express the transcription factor GATA-3 and produce type 2 cytokines, especially IL-5 and IL-13. ILC2 surface markers include CD127, CRTh2, CD161, and CD25 (IL-2Rα), and these systemically distributed cells have an important role during infection (by viruses, parasites), in atopic conditions (allergy, airway hyperresponsiveness), and tissue repair.[9-11] Group 3 ILCs (ILC3s) express the orphan nuclear receptor RORγt and produce IL-17A and IL-22 after stimulation. ILC3s play important roles in maintaining barrier surfaces (especially mucosal sites) and for protection against infections by fungi and extracellular bacteria. Interestingly, ILC3s are deregulated in inflammatory conditions (irritable bowel disease, psoriasis), suggesting that this subset may be involved with disease.[12-14]

In principle, HIS mouse models can provide an opportunity to better understand the development, differentiation, and function of human ILCs in vivo. Along these lines, several reports have described human NK cell generation in HIS mice[15-18] and have underscored the importance of species-specific cytokines and macrophage tolerance for the development and function of these innate effectors.[15] In contrast, reports on other human ILC subsets in humanized mice are scarce and only in the context of inflammation.[19,20] Several ILC subsets inhabit mucosal tissues, and the reconstitution of these sites in most humanized mouse models appears rather limited (reviewed in Ito et al[21]). This may result from poor homing or maintenance of human hematopoietic cells because of incompatibilities in adhesion molecules, chemokine/chemokine receptors, and/or growth and survival factors. A comprehensive analysis of human ILCs in HIS mice could provide new insights into how, when, and where these cells develop.

Previous studies correlated FMS-related tyrosine kinase 3 ligand (Flt3L)-mediated expansion of mouse dendritic cells (DCs) with a higher ILC cell survival and proliferation.[22-25] We recently reported a humanized mouse model in which Flt3L-mediated enhancement of human DC numbers resulted in improved human NK cell homeostasis.[26] In this report, we generate and characterize a novel BALB/c *Rag2*$^{-/-}$*Il2rg*$^{-/-}$*Sirpa*^{NOD}*Flk2*$^{-/-}$ (BRGSF) HIS mouse model with enhanced human ILC homeostasis and function. We provide evidence for a functional "cross talk" between human DC and human ILC subsets that occurs in across lymphoid and nonlymphoid (mucosal) tissues. BRGSF-based HIS mice should provide the means to interrogate human ILC function in the context of infection and inflammation.

Materials and methods

Generation of HIS mice in a novel BRGF recipient strain

BRGSF mice were generated by extensive backcrossing of BALB/c *Rag2*$^{-/-}$*Il2rg*$^{-/-}$*Flk2*$^{-/-}$ (BRGF; see Li et al[26]) mice to the BALB/c *Rag2*$^{-/-}$*Il2rg*$^{-/-}$*Sirpa*^{NOD} strain.[15] BALB/c *Rag2*$^{-/-}$*Il2rg*$^{-/-}$*Sirpa*^{NOD}*Flk2*$^{+/-}$ mice were subsequently intercrossed to create the BRGSF strain. HIS mice were generated as previously described.[15,16] Briefly, fetal liver CD34^{+} cells were isolated using human CD34 microbead kit (Miltenyi Biotec) and subsequently phenotyped for CD38 expression by flow cytometry. Newborn (3 to 5 days of age) received sublethal irradiation (3 Gy) and were injected intrahepatically with the equivalent of 2×10^5 CD34^{+}CD38^{-} human fetal liver cells. All manipulations of HIS mice were performed under laminar flow conditions. Experiments were approved by the ethical committee at the Institut Pasteur (reference no. 2007-006) and validated by the French Ministry of Education and Research (reference no. 02162.02).

In vivo Flt3L treatment

HIS mice were injected intraperitoneally (IP) 3 times per week for 2 weeks with 5 μg hFlt3L-Fc (BioXcell), commencing at 6 to 7 weeks after reconstitution. Control mice were injected with the same volume of phosphate-buffered saline (PBS). HIS mice were analyzed 2 to 5 days after the last hFlt3L injection.

Hydrodynamic injection

Full-length human IL-2, IL-7, IL-25, and IL-33 complementary DNA clones were cloned in the mammalian cell expression vector pCMV-6-XL4 (Origene) and plasmids purified using the endotoxin-free Plasmid-Maxi kit (Qiagen). Hydrodynamic injection in HIS mice was performed as previously described.[27] Briefly, 8- to 9-week-old HIS mice were weighed and injected IV (tail vein) with cytokine encoding plasmids in 1.8 mL PBS (for 20 g body weight) within 7 seconds using 27-gauge needles.

Cell preparation

HIS mice were perfused with PBS before tissue preparation. Spleen tissue was minced and erythrocytes were lysed (BD Bioscience). Percoll density gradient centrifugation (GE Healthcare Life Sciences) was used for liver lymphocyte preparation. Lungs were dissociated using 1 mg/mL collagenase D (Roche) for 45 minutes followed by Percoll density gradient centrifugation.

Small and large intestines were perfused with cold RPMI 1640 medium to remove feces, cut open longitudinally, and washed. Pooled tissue was cut into 1-cm pieces and agitated in prewarmed medium containing 10 mM EDTA (Sigma-Aldrich) at 37°C for 30 minutes to remove epithelial cells. The remaining tissue was collected, minced, and digested for 60 minutes in medium containing 5% fetal calf serum and Liberase (1 mg/mL; Roche). Lamina propria lymphocytes were enriched by Percoll gradient centrifugation, filtered, and washed. All cell preparation steps were performed using RPMI 1640 Glutamax (Life Technologies) 100 U/mL penicillin and 100 μg/mL streptomycin (Invitrogen) unless otherwise stated.

Flow cytometry

Cells were incubated for 15 minutes with cold PBS (Life Technologies) containing 3% fetal calf serum, human and mouse FcR block (hIgG and 2.4G2), and a viability dye (eFluor 506; eBioscience #65-0866-14). After a washing step, cells were stained with fluorochrome-bound antibodies. To detect intracellular transcription factors and cytokines, cells were subsequently fixed and permeabilized using manufacturer's protocols (eBioscience; BD). Antibodies used are listed in supplemental Table 1. Samples were acquired using an LSR FORTESSA (BD); data were analyzed using FlowJo software (TreeStar; versions 9.8.5 and 10.0.8).

In vitro stimulation assays

For ex vivo stimulation assays, human ILCs were enriched by depletion of cells expressing mCD45, hCD3, hCD5, and hCD19 using magnetic cell separation (Miltenyi Biotec) according to the manufacturer's procedures. ILCs were plated in 96-cell plates at a density of 4×10^4 NK cells (hCD45^{+}CD3^{-}NKp46^{+}) or 10^4 ILCs

(hCD45$^+$Lin$^-$CD7$^+$CD127$^+$) per well. Cells were stimulated using various cytokines (including IL-15 [Peprotech], IL-12, IL-18, IL-23, IL-1b, IL-33, and IL-25 [R&D Systems]) at a concentration of 50 ng/mL and in the presence of Golgi Plug (BD) for 4 hours. In some cases, stimulation was performed with phorbol 12-myristate 13-acetate (10 ng/mL; Sigma-Aldrich) plus ionomycin (1 μg/mL; Sigma-Aldrich) in the presence of Golgi Plug (BD) for 3 hours. For degranulation assays, anti-CD107a antibody and monensin (1 μg/mL; Sigma-Aldrich) was added to the media 1 hour after the beginning of the stimulation (1 μL/well). In all cases, a nonstimulated control containing only medium was included.

In vivo stimulation assays

For NK stimulation, reconstituted HIS mice were injected IP with 50 μg poly(I:C) (InvivoGen) in PBS and analyzed 14 hours later. For ILC stimulation, a cocktail of flagellin, R848 (Resiquimod), and bacterial lipopolysaccharide (LPS-EB ultrapure) (all from InvivoGen, 5 μg each) was injected IP and analyzed 6 hours later.

Statistical analysis

GraphPad Prism, version 6 (GraphPad Software), was used to perform statistical analysis. Statistical significance was evaluated by 2-tailed unpaired Student *t* tests. The obtained *P* values were considered significant when $< .05$.

Results

Human DC development in Flt3L-treated BRGSF-based HIS mice

We have previously described BRGF recipients that offer an approach to enhance human DC homeostasis in HIS mice[26] and characterized the BALB/c *Rag2*$^{-/-}$*Il2rg*$^{-/-}$*Sirpa*^{NOD} strain with enhanced human hematopoietic engraftment resulting from improved macrophage tolerance of human cells.[15] We combined these 2 models to create the BRGSF strain and analyzed HIS mice after intrahepatic transfer of human CD34$^+$ HSCs into newborn BRGSF recipients. BRGSF-based HIS mice showed robust reconstitution, with up to 75% circulating human CD45$^+$ cells (supplemental Figure 1A), including CD3$^+$ T cells (5% to 30%), CD19$^+$ B cells (60% to 85%), NK cells (2% to 6%), and conventional DCs (cDCs) (1% to 4%) (supplemental Figure 1A). Consistent with previous studies,[26,28-31] we found that exogenous Flt3L treatment could significantly boost human myeloid cell development in BRGSF HIS mice (Figure 1). We examined 4 human CD3$^-$CD19$^-$NKp46$^-$HLA-DR$^+$ myeloid subpopulations: CD14$^+$ monocytes, CD123$^+$ plasmacytoid DCs (pDCs), CD141/BDCA-3$^+$ cDCs, and CD1c/BDCA-1$^+$ cDCs. All 4 subsets were detected in BM (Figure 1A) and spleen (Figure 1C) and to a lesser extent in lung and liver (data not shown) of BRGSF HIS mice as minor populations (1% to 5%) of total CD45$^+$ cells. Flt3L treatment resulted in a 30- to 85-fold increase in absolute numbers of these myeloid subsets in the BM and a threefold increase in absolute numbers of pDCs and CD141$^+$ DCs in the spleen (Figures 1B,D). Exogenous Flt3L had no effect on the Flt3-deficient mouse myeloid cells (data not shown), thereby allowing a selective boost of human myeloid cells in this context. Compared with previous studies using BRGF recipients,[26] we found a quantitatively stronger effect in the absolute numbers that was further extrapolated to CD14$^+$ monocytes and localized not only in spleen but systemically.

We next analyzed hematopoietic and myeloid precursor populations in the BM of reconstituted BRGSF HIS mice. Total numbers of CD34$^+$ HSCs were significantly higher in Flt3L-treated mice, suggesting enhanced homeostasis (supplemental Figure 2A). This is in line with previous in vitro and in vivo studies demonstrating that HSCs express Flt3 and that signaling through this receptor induces proliferation of quiescent BM HSCs and positively affects cell survival.[32,33] Human DC/monocyte restricted precursors (Lin$^-$CD34$^-$CD117$^+$CD135$^+$CD116$^+$CD45RA$^+$ fraction) have been shown to have a BM origin before entry into the circulation.[34,35] This population was detected in the BM of BRGSF mice (supplemental Figure 2B), and its frequency and total numbers increased following Flt3L treatment (supplemental Figure 2C). These data suggest that the increased frequency and absolute numbers of myeloid cells in Flt3L-treated BRGSF HIS mice may result from an increase in the CD34$^+$ HSC pool and their downstream DC/monocyte precursors within the BM that expand in response to exogenous Flt3L.

Lymphocyte development in Flt3L-treated BRGSF HIS mice

We next analyzed development of B and T cells in BRGSF HIS mice receiving or not receiving Flt3L. T-cell development as assessed by total thymocyte numbers, and CD4/CD8 profiles were similar to previous reports and unaffected by Flt3L treatment (supplemental Figure 3A). Splenic T-cell frequencies and CD4/CD8 ratios were not significantly affected by Flt3L treatment, and their phenotypic profiles were unchanged and consisted of a majority of the cells presenting a naïve phenotype (CD45RA$^+$CD27$^+$), around 20% being central memory (CD45RA$^-$CD27$^+$) and a minority (<10%) expressing markers of effector functionality (supplemental Figure 3B). BM B-cell maturation was not affected by the treatment, and we observed B precursor CD19$^+$ and CD19$^+$CD20$^+$ cells and mature IgD$^+$IgM$^+$ cells at analogous frequencies (supplemental Figure 3C).

Given previous studies demonstrating the effect of DC cross talk in promoting NK cell maturation and proliferation,[24,26] we tested whether Flt3L-dependent enhancement of myeloid cell development in BRGSF HIS mice affected the phenotype and function of conventional NK cells (defined as CD3$^-$NKp46$^+$CD94$^+$ cells). Administration of Flt3L to BRGSF mice led to an increase in frequency and absolute number (2- to 2.5-fold) of conventional NK cells in the liver, spleen, and lung (Figures 2A,B), as well as in blood, BM, and intestine (data not shown). Conventional NK cells in humans include 2 main subsets: a CD56^{bright}CD16$^-$ and a more mature CD56^{dim}CD16$^+$ subset (reviewed in Cooper et al[36]). As reported in other HIS mouse models,[17,26] the majority of CD56$^+$ NK cells in BRGSF HIS mice were CD16$^-$, with about 30% expressing the low-affinity Fc receptor (Figure 2C). Flt3L treatment did not change the proportions of CD16$^+$ NK cells (Figure 2C) or the expression pattern of the C-type lectin receptors NKG2A and NKG2C (Figure 2D). Major histocompatibility complex class I–specific KIR expression was restricted to the CD16$^+$ subsets and accounted for 15% to 30% of the total CD94$^+$ population depending on the organ (Figure 2E, left). Both activating (KIR2DS4) and inhibitory KIR (KIR2DL1/DL2/DL3) molecules were expressed, suggesting a balanced repertoire formation on NK cells. Neither the percentage of KIR-expressing NK cells nor the ratio of activating vs inhibitory receptors was affected by Flt3L treatment (Figure 2E, right).

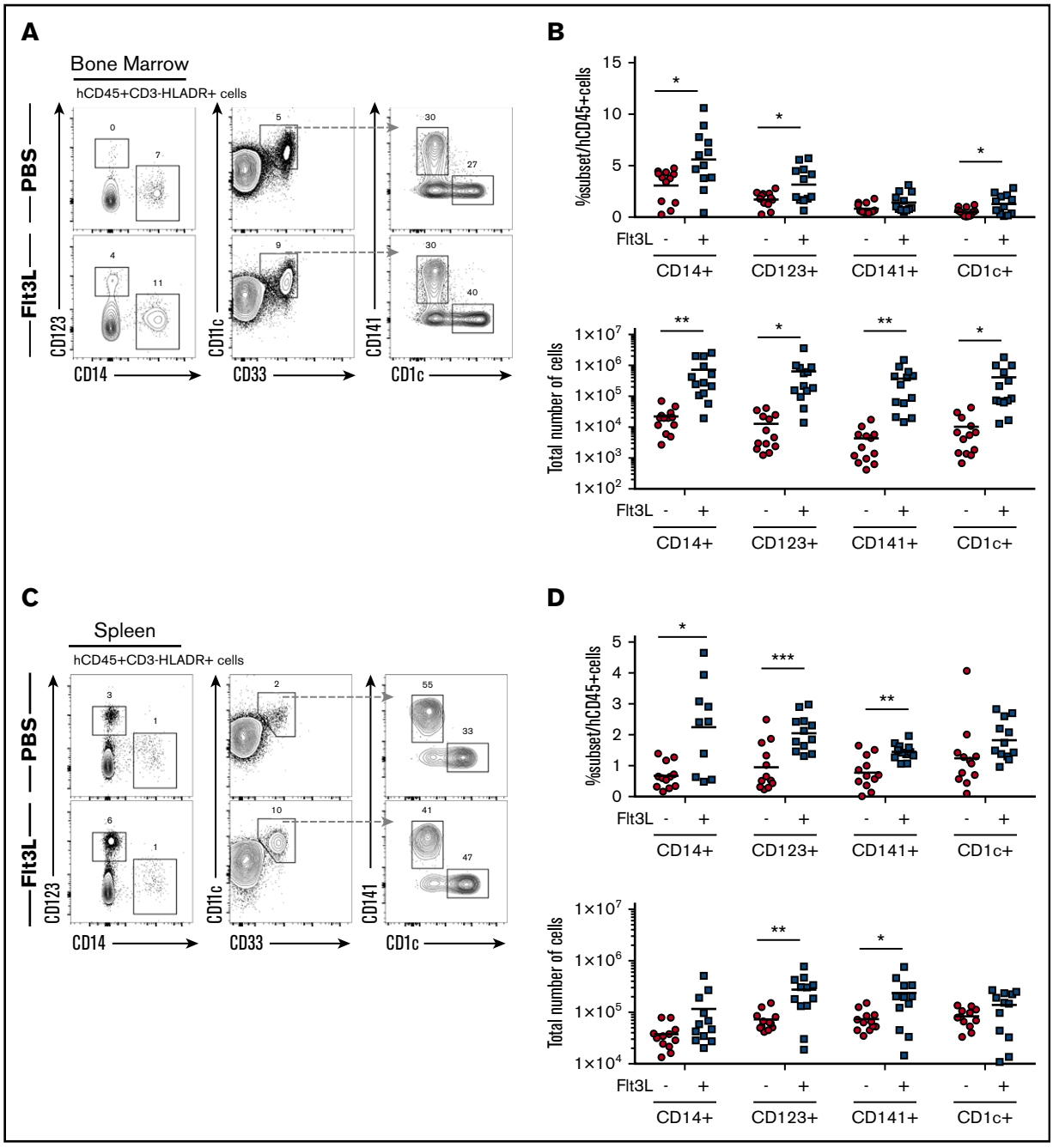

Figure 1. Distribution of human myeloid subsets in BRGSF mice and effect of Flt3L on their development. Representative flow cytometry immunophenotypic analysis of hCD45$^+$HLA$^-$DR$^+$CD19$^-$CD3$^-$CD56$^-$ cells from bone marrow (A) and spleen (C) of an Flt3L-treated mouse and a PBS-treated littermate engrafted with the same CD34$^+$ HSC donor. Comparison of frequencies within the human CD45$^+$ cells and total number of the 4 myeloid subsets (CD14$^+$ monocytes, CD123$^+$ pDCs, CD141$^+$ cDCs, and CD1c$^+$ cDCs) with or without Flt3L treatment in bone marrow (B) and spleen (D). Each dot represents 1 mouse. Composite data from 3 independent experiments are shown. Numbers in plots represent frequencies within gates.

NK cell priming following Flt3L-mediated human DC boost

Because IL-15 transpresentation by DCs has been shown to prime resting NK cells,[37,38] we compared the cytokine production and degranulation capacity of NK cells in BRGSF HIS mice with or without Flt3L-mediated DC boost. Splenic NK cells were stimulated with IL-12, IL-15, and IL-18 ex vivo, and IFN-γ production was assessed by intracellular staining (Figure 3A, top). Flt3L treatment increased the frequency of IFN-γ–producing NK cells compared with control mice (Figure 3B). In contrast, NK cell degranulation (CD107a expression) upon cytokine activation was not altered in Flt3L-treated mice. To assess DC-NK cell cross talk in vivo, we stimulated DCs via TLR3 following IP injection of poly(I:C) and assessed NK cell cytokine production ex vivo 14 hours later. DC

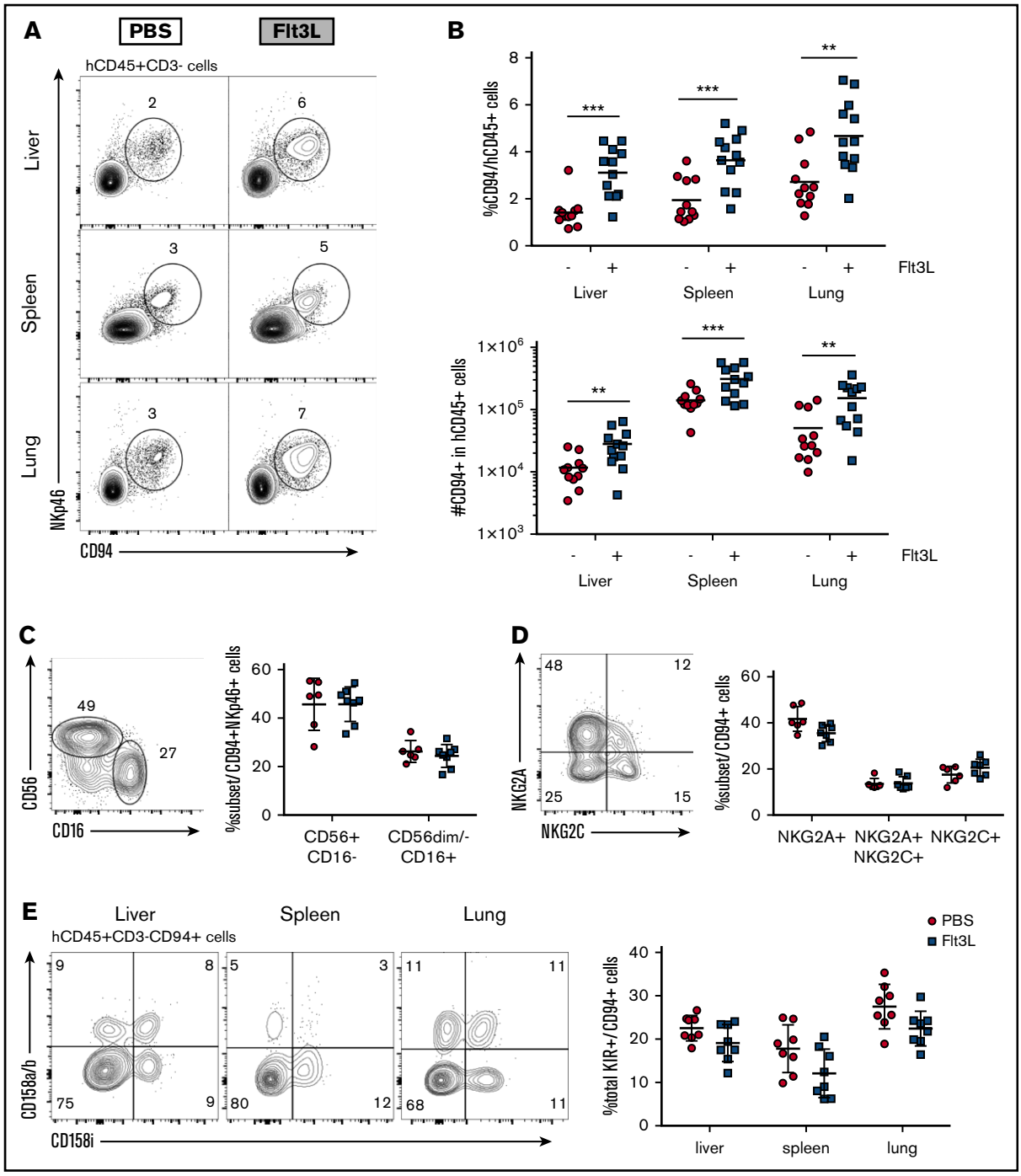

Figure 2. Distribution of human NK cells in reconstituted BRGSF mice with or without Flt3L treatment. (A) Representative flow cytometry immunophenotypic analysis of alive hCD45$^+$CD3$^-$CD94$^+$NKp46$^+$ NK cells from liver, spleen, and lung of an Flt3L-treated mouse and a PBS-treated littermate engrafted with the same CD34$^+$ HSC donor. (B) Comparison of CD94$^+$ cell frequencies within the human CD45$^+$ cells (top) and total number of NK cells (bottom) with or without Flt3L treatment in liver, spleen, and lung. (C) Representative flow cytometry plot of CD56 and CD16 expression in liver NKp46$^+$CD94$^+$ cells as gated in top panels (left) and comparative quantification (right). (D) Expression of NKG2A and NKG2C in liver NKp46$^+$CD94$^+$ cells (left) and comparative quantification (right). (E) Distribution of activating (CD158i) and inhibitory (CD158a/b) KIR expression in liver, spleen, and lung NK cells of a representative BRGSF mouse treated with Flt3L (left) and comparative quantification of the total KIR-expressing CD94$^+$ NK cells with or without Flt3L treatment (right). Each dot represents 1 mouse. Composite data from at least 3 independent experiments are shown. Numbers in plots represent frequencies within gates.

activation through TLR was confirmed by IL-12 levels in plasma of mice before the beginning of the Flt3L treatment, after the Flt3L treatment but before the poly(I:C) injection and 14 hours later, and when mice were analyzed (supplemental Figure 4). We found that BRGSF HIS mice receiving Flt3L treatment demonstrated enhanced NK cell IFN-γ production and a marked increase in CD107a expression in response to poly(I:C) activation (Figure 3C). Although these responses were also observed in

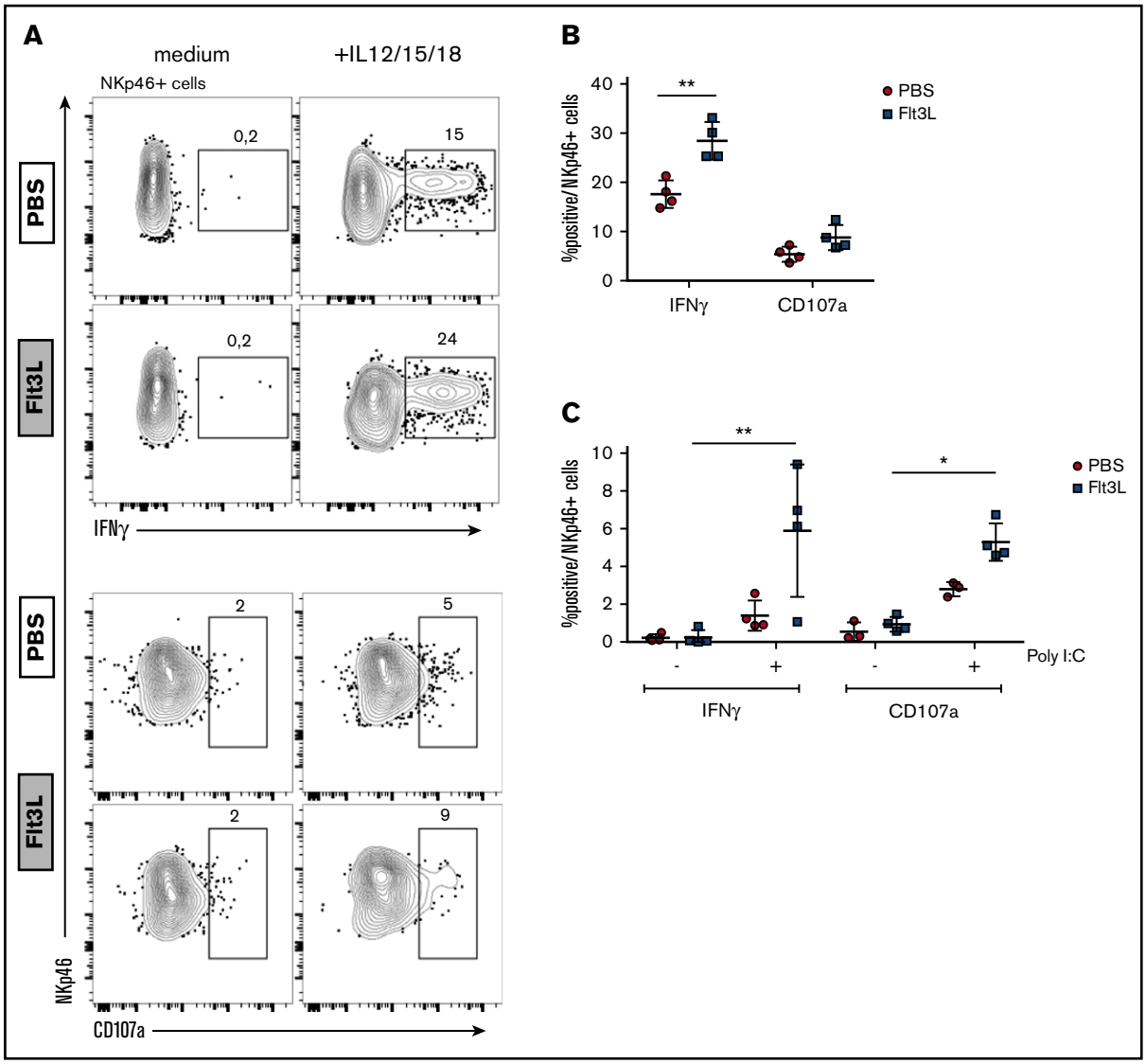

Figure 3. Flt3L treatment enhances human NK cell function in spleen cells from reconstituted BRGSF mice. (A) Human NK cells were magnetic-activated cell sorting–enriched from spleens of BRGSF Flt3L treated or not and were stimulated ex vivo with the monokines IL-12, IL-15, and IL-18. Representative flow cytometry immunophenotypic analysis of degranulation (CD107a) and cytokine production (IFN-γ) in NKp46$^+$ NK cells is shown. (B) Quantification of IFN-γ–producing and CD107a-expressing NK cells from Flt3L-treated or control BRGSF mice. (C) In vivo functionality of NK cells in BRGSF mice was evaluated by quantifying IFN-γ production and degranulation after in vivo poly(I:C) stimulation. (B,C) Composite data of 4 mice per condition in 2 experiments. Each dot represents 1 mouse. Numbers in plots represent frequencies within gates.

BRGSF HIS mice that had not been Flt3L-boosted, the amplitude of the NK cell response was significantly higher in Flt3L-treated HIS mice. These results suggest that increased human DCs in Flt3L-boosted BRGSF HIS mice can be stimulated in vivo and "transactivate" effector functions in NK cells. Direct signaling of TLR agonists on TLR expressing NK cells[39] may contribute to the enhancement.

Administration of Flt3L enhances development of diverse ILC subsets in BRGSF mice

ILCs include several subsets of lineage$^-$CD127$^+$ cells that have the capacity to rapidly produce cytokines in the early phases of immune responses (reviewed in Eberl et al[40]). We next assessed the impact of Flt3L treatment in BRGSF mice on the development of ILC (defined as lineage$^-$EOMES$^-$CD7$^+$CD127$^+$ cells). ILCs were detected in liver, spleen, lung, and gut and accounted for 0.5% to 2% of the total hCD45$^+$ cells in these organs (Figure 4A). Administration of Flt3L increased both the ILC frequency (Figure 4A) and absolute numbers (Figure 4B) in all organs tested, with the most pronounced effects in the liver and gut. Interestingly, Flt3 receptor (CD135) was not expressed by ILCs in spleen, liver, and lung, ruling out the direct signaling of Flt3L on these cells (supplemental Figure 5).

Diverse TBET$^+$ IFN-γ–producing ILC subsets have been reported in various locations and with diverse, sometimes overlapping, surface markers (reviewed in Spits et al[41]). We next assessed ILC1 heterogeneity in BRGSF mice, focusing on the liver, where several CD127$^+$ ILC1 populations distinct from NK cells have been

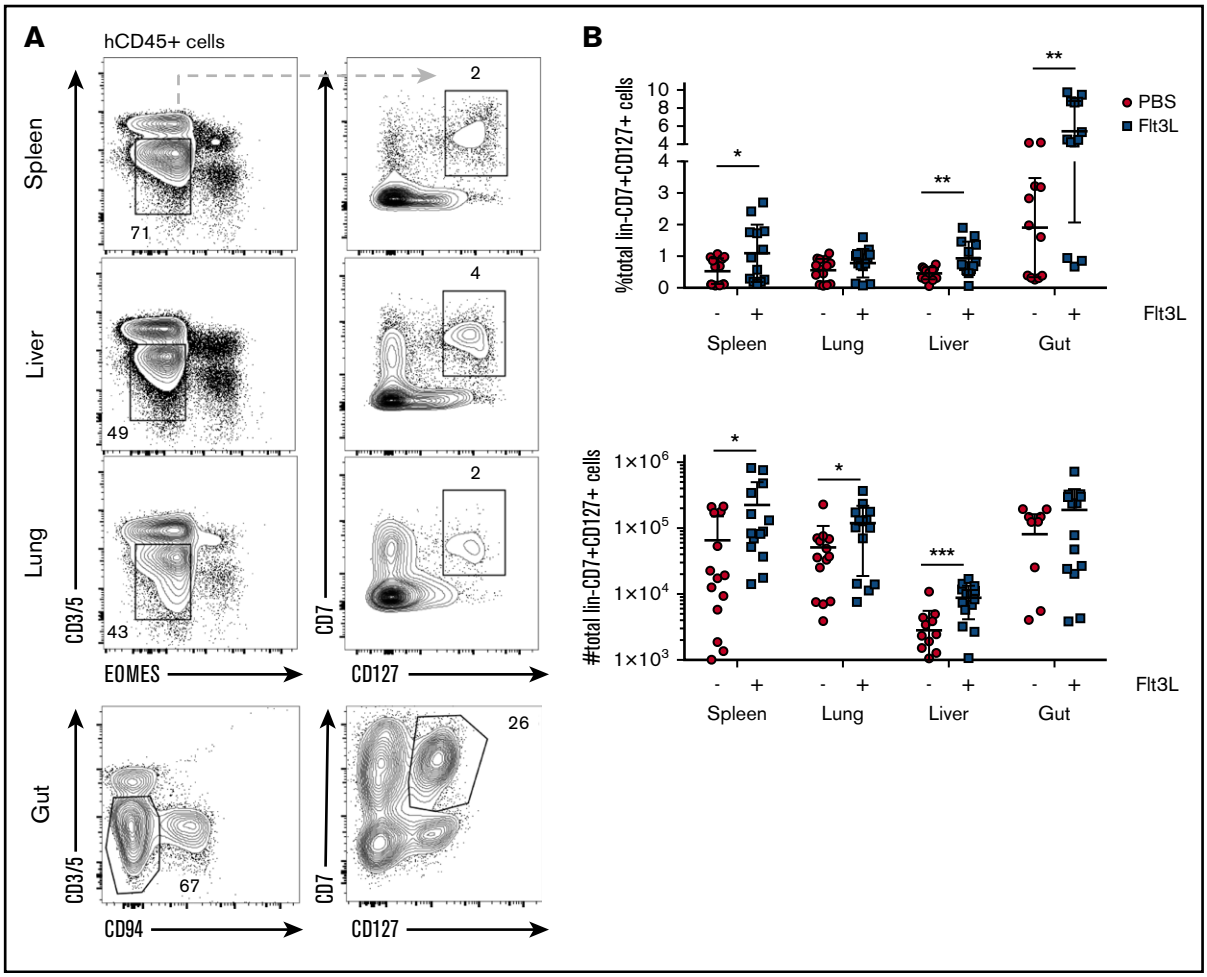

Figure 4. Distribution of human ILCs in BRGSF mice and effect of Flt3L treatment. (A) Representative flow cytometry analysis of CD3$^-$CD5$^-$EOMES$^-$CD7$^+$CD127$^+$ innate lymphoid cells in spleen, liver, and lung and CD3$^-$CD5$^-$CD94$^-$CD7$^+$CD127$^+$ cells in gut of an Flt3L-treated BRGSF mouse. (B) Comparative quantification of ILCs in spleen, lung, liver, and gut of BRGSF mice treated or not with Flt3L as a percentage of hCD45$^+$ cells (top) and total number of cells (bottom). Composite data from of 14 mice per condition in 4 experiments are shown. Each dot represents 1 mouse. Numbers in plots represent frequencies within gates.

reported.[19,42,43] BRGSF mice harbor 2 TBET$^+$ lineage$^-$CD7$^+$ populations that can be distinguished on the basis of IL7Rα (CD127) expression (Figure 5A). TBET$^+$CD127$^-$ cells represent conventional NK cells and coexpress EOMES, CD161, and high levels of CD94 (Figure 5B). In contrast, a second TBET$^+$CD127$^+$ subset could be detected that also expressed CD161 and EOMES, but showed an essentially negative expression of CD94 (Figure 5B). These TBET$^+$CD127$^+$ cells did not express the NK marker CD16 and had lower expression of NKp46 than conventional NK cells (Figure 5C). This ILC1 subset accounted for <0.1% of hCD45$^+$ liver cells, similar to a recently described human intrahepatic NK-like ILC.[44] Flt3L treatment increased the frequency and absolute numbers of these hepatic ILC1s (Figure 5D).

We next addressed the IFN-γ production capacity of Lin$^-$CD7$^+$ TBET$^+$ cells upon ex vivo stimulation. Both TBET$^+$CD127$^+$ ILC1 and conventional TBET$^+$CD127$^-$ NK cells showed strong IFN-γ production after pharmacological activation (Figure 5E). We further showed that CD161$^+$ ILC1s could be activated following TLR triggering in vivo (using a TLR-4, TLR-5, TLR-7, and TLR-8 ligand cocktail of flagellin, lipopolysaccharide, and R484). Flt3L-treated BRGSF HIS mice were TLR-stimulated treated or not;16 hours later, hepatic lymphocytes were stained for intracellular IFN-γ. We found that TLR stimulation was able to stimulate an IFN-γ response in CD161$^+$ liver ILCs above levels observed in non-TLR–stimulated mice (Figure 5F), suggesting that DC activation via TLR stimulation is able to "transactivate" hepatic ILC1s in vivo.

Increased lung ILC2 homeostasis in Flt3L-treated BRGSF HIS mice

We next studied the impact of Flt3L treatment on other ILC subsets. ILC2s are present at mucosal sites and play a key role in barrier protection in the respiratory tract (reviewed in Bernink et al[45]). We detected human ILC2s in the lung of BRGSF HIS mice as a population of lineage$^-$CD7$^+$CD127$^+$TBET$^-$EOMES$^-$GATA-3$^+$ cells (Figure 6A). The frequency and absolute numbers of ILC2 within the lung of BRGSF HIS mice was increased by Flt3L treatment (Figure 6B). On average, GATA-3$^+$ ILC2s represented ~0.35% of the human CD45 cells within the lung.

We found that ILC2s in the lungs of BRGSF HIS mice had phenotypic similarities to ILC2s from human tissues, with notable

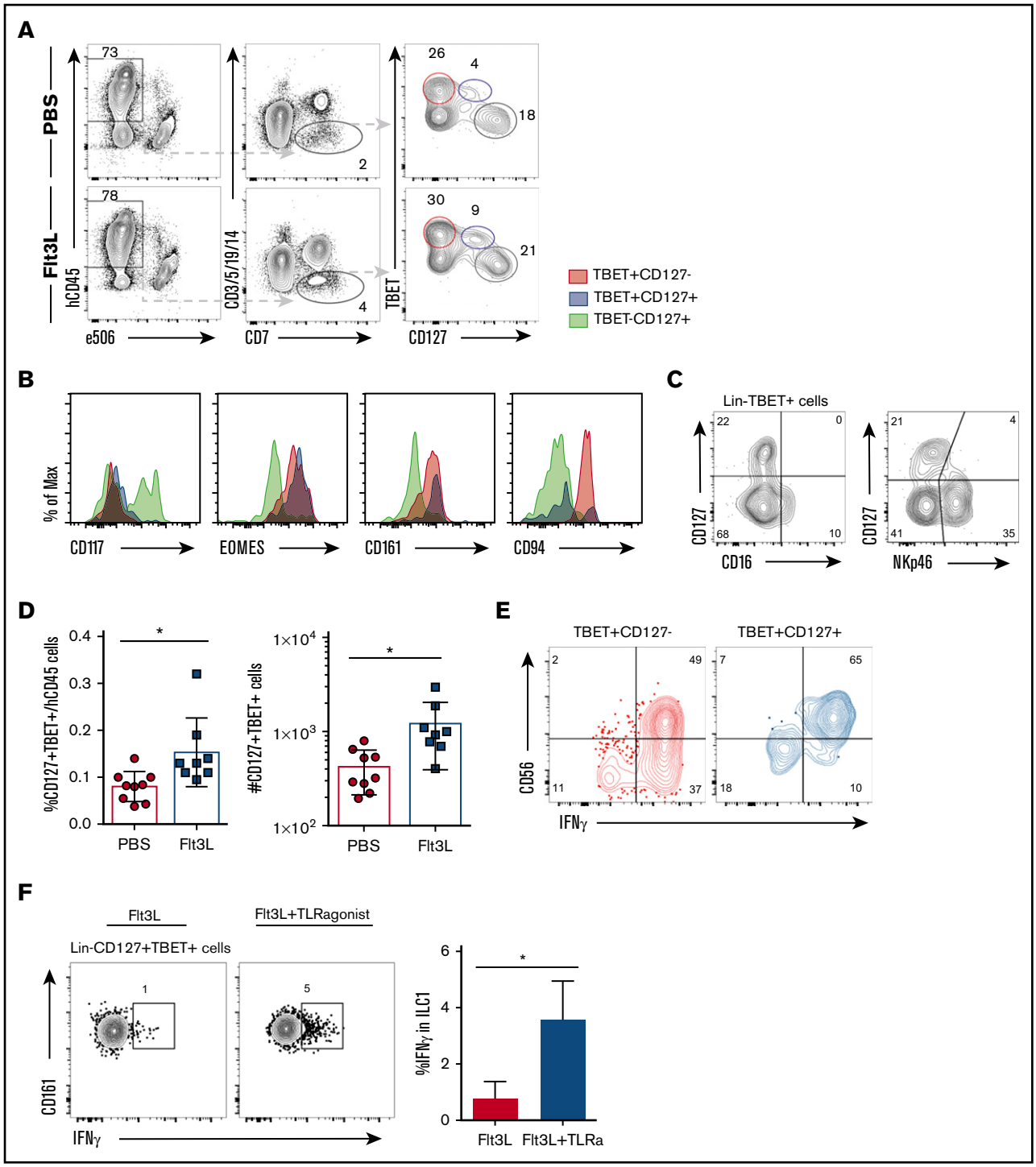

Figure 5. Flt3L treatment expands a population of ILC type 1 cells differently from NK cells. (A) Representative flow cytometry analysis of TBET and CD127 expression on Lin$^-$CD7$^+$ cells in liver of a PBS- and a littermate Flt3L-treated BRGSF mouse. (B) Expression of CD117, EOMES, CD161, and CD94 (histograms) on liver TBET$^+$CD127$^-$ (red), TBET$^+$CD127$^+$ (blue), and TBET$^-$CD127$^+$ cells (gray) assessed by flow cytometry. (C) Expression of CD127, CD16, and NKp46 on liver Lin$^-$TBET$^+$ cells, assessed by flow cytometry. (D) Frequency among hCD45$^+$ cells (left) and total number (right) of Lin$^-$CD7$^+$CD127$^+$TBET$^+$ liver cells. (E) Representative functional analysis by IFN-γ intracellular flow cytometry after phorbol 12-myristate 13-acetate/ionomycin plus cytokine 4-hour stimulation of TBET$^+$CD127$^-$ (red) and TBET$^+$CD127$^+$ (blue) cells. Gated cells were determined using unstimulated controls. (F) Flow cytometry representation of IFN-γ production by Lin$^-$CD127$^+$TBET$^+$CD161$^+$ ILC1 cells in response to TLR-mediated in vivo stimulation. Composite data from of 3 to 4 mice per condition are shown at left. Numbers in plots represent frequencies within gates.

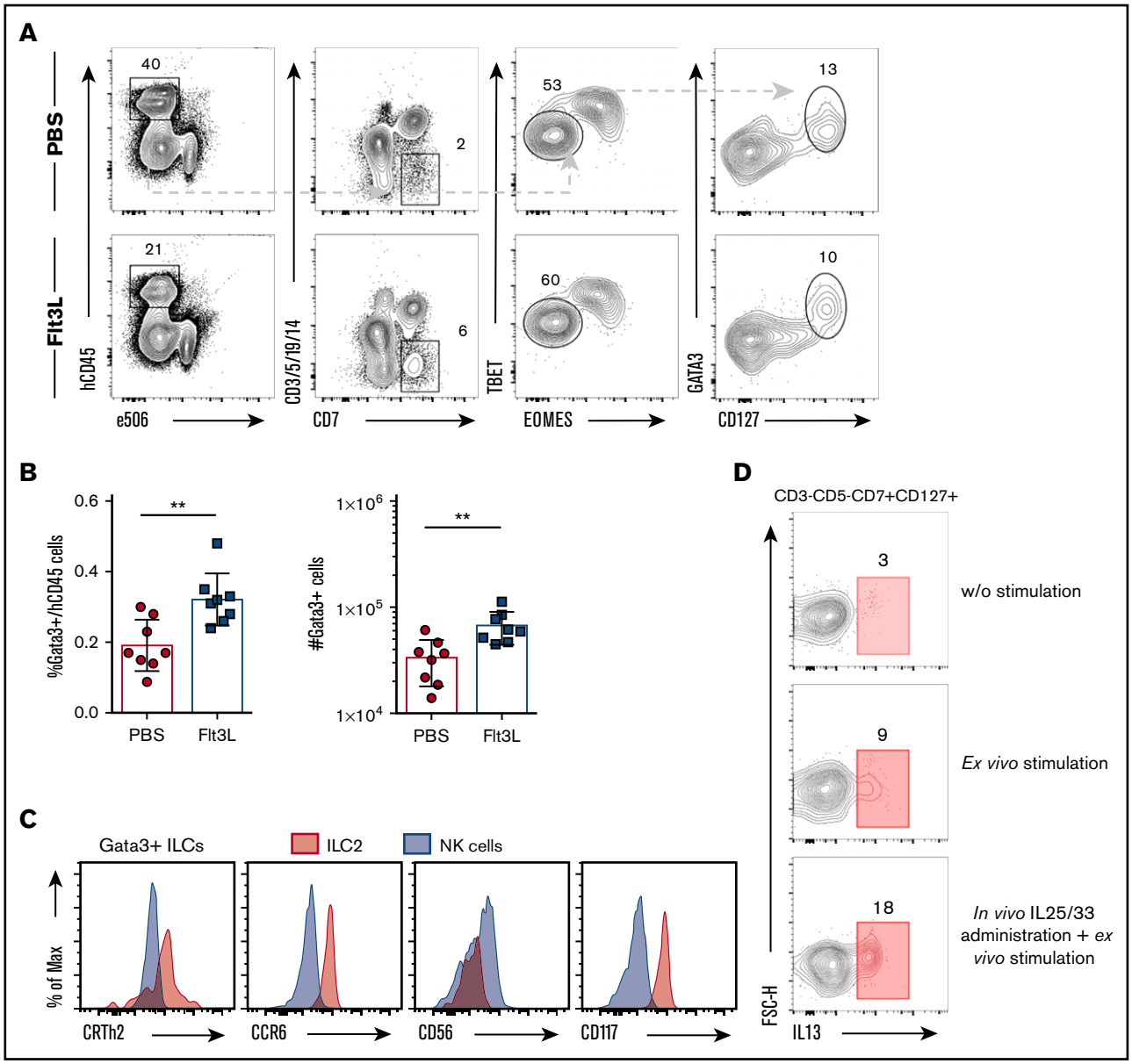

Figure 6. Flt3L treatment also augments ILC type 2 cells in reconstituted BRGSF mice. (A) Representative flow cytometry analysis of GATA-3$^+$ ILCs in lung of reconstituted BRGSF mice treated or not with Flt3L. (B) Frequency among hCD45$^+$ cells and total number of GATA-3$^+$ ILCs in lung of reconstituted BRGSF mice treated or not with Flt3L. Composite data from 8 mice of 2 experiments is shown. (C) Representative functional analysis by IL-13 intracellular flow cytometry from freshly isolated lung ILCs, after P/I ex vivo stimulation, and after in vivo hydrodynamic cytokine injection and ex vivo stimulation. (D) Expression of CRTh2, CCR6, CD56, and CD117 (histograms) on lung GATA-3 ILCs (red) and EOMES$^+$TBET$^+$ NK cells (gray) assessed by flow cytometry. Each dot represents 1 mouse. Numbers in plots represent frequencies within gates. Max, maximum; w/o, without.

expression of the prostaglandin D2 receptor CRTh2, c-kit receptor (CD117), the chemokine receptor CCR6, and low or negative expression of CD56[46-48]) (Figure 6C). Lung ILC2s in BRGSF HIS mice showed detectable IL-13 production under steady-state conditions that could be increased after ex vivo stimulation with phorbol 12-myristate 13-acetate/ionomycin (Figure 6D). To assess the impact of survival factors and inflammatory cytokines on human ILC2 function in vivo, we administrated in vivo a cocktail of human cytokines (IL-2, IL-7, IL-25, and IL-33) by hydrodynamic injection and assessed IL-13 production capacity 6 days later. Following in vivo cytokine expansion and stimulation, we found that a substantial proportion of ILC2s expressed IL-13 (Figure 6D). These results suggest that human ILC2s in BRGSF HIS mice are cytokine responsive in vivo and that ILC2 function can be primed under appropriate environmental conditions.

Flt3L stimulates intestinal ILC homeostasis and function in BRGSF HIS mice

ILC3s are enriched in intestinal lamina propria and play a fundamental role in gut homeostasis and immune defense. Human CD45$^+$ cell engraftment in the gut was quite variable in individual

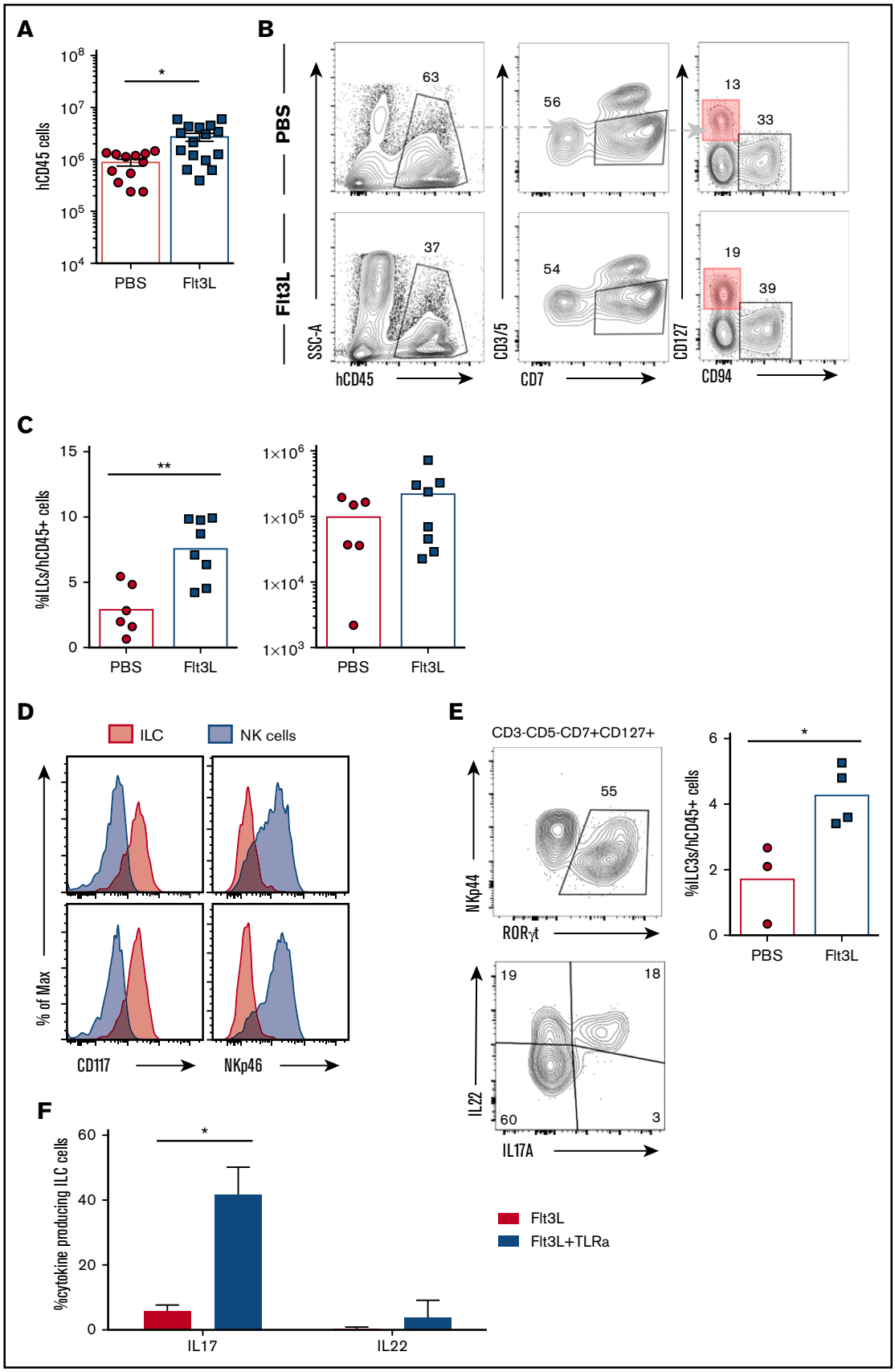

Figure 7.

BRGSF HIS mice (Figure 7A), ranging from nonreconstitution to 6×10^6 hCD45$^+$ cells in intestinal lamina propria. In reconstituted HIS mice, gut lamina propria cells included T cells (4% to 20%), CD94$^+$ NK cells (3% to 15%), and a clearly detectable subset of lineage$^-$CD7$^+$CD127$^+$ ILCs (1% to 5%). These intestinal ILCs expressed CD117 but were negative for NKp46 (Figure 7D) and therefore resembled NCR$^-$ ILC3s previously described in diverse human tissues.[19,49] Flt3L administration resulted in an increase of the frequency of gut ILC3s (reaching, in some cases, 10% of the total hCD45$^+$ cell population) that was accompanied by an increase in total ILC number (Figures 7B,C). Intestinal ILC3s in BRGSF HIS mice expressed the transcription factor RORγt and, following in vitro simulation, were able to produce IL-22 and IL-17A (Figure 7E). When human DCs were stimulated in vivo with a cocktail of TLR ligands (see the previous section), we found that intestinal ILC3s showed a modest increase of IL-22 production with no impact from the Flt3L treatment (Figure 7F). However, IL-17A was drastically boosted after stimulation, and that increase was even more prominent in the Flt3L-treated mice, suggesting a positive effect of the ligand on the functional fitness of ILC3 in vivo. Whether this effect is exclusively mediated by DC stimulation or via direct TLR signaling on ILCs[50] will require further study.

Discussion

ILCs play fundamental roles in early immune response against diverse pathogens and in later stages of infection and inflammation through promotion of tissue homeostasis and repair. As such, ILC activation and regulation may affect disease outcome in some clinical conditions. The development of suitable small-animal models that recapitulate ILC development and function in vivo could provide a preclinical testing platform to assess immunomodulatory approaches that target ILCs. Here we show that Flt3L-boosted BRGSF recipients provide a simple HIS mouse model for robust generation of diverse human innate and adaptive lymphocyte subsets. In particular, we find that mature, functional human ILC subsets are present in lymphoid and nonlymphoid tissues of BRGSF HIS mice, thereby opening a path to understanding human ILC immunobiology in vivo in the context of infection, inflammation, and cancer.

Two nonexclusive mechanisms may underlie the ability of Flt3L-boosted BRGSF HIS mice to robustly develop human ILCs. Because Flt3L regulates early DC precursors and homeostasis[22-26] (Figure 1; supplemental Figure 2), an improved myeloid compartment may provide a richer human cytokine environment,[51] thus indirectly supporting ILC survival and proliferation. This mechanism underlies DC transpresentation of IL-15 to mouse and human NK cells.[16,24,37] A second mechanism may involve direct effects of Flt3L on CD135$^+$ lymphoid committed precursors that are upstream of human ILC or NK precursors.[52-54] These 2 pathways may act synergistically to contribute to the observed human ILC boost in BRGSF HIS mice. NK cells engage in bidirectional interactions with other innate effectors that modulate their differentiation, homeostasis, and immune responses against pathogens and cancer.[55] This innate cross talk can further impact adaptive responses, as evidenced by the reduced benefit of DC vaccination after NK cell depletion in a melanoma mouse model.[56] Both soluble (IFN-γ) as well as contact-dependent (OX40-OX40L) factors contribute to NK cell–DC immune orchestration. These interactions may underlie the increased cytokine production and degranulation capacity we observe in BRGSF mice. Because both myeloid and NK cells are expanded in BRGSF HIS mice, our model provides an opportunity to study the importance of this cross talk in human innate immunity.

The robust ILC development we observed in BRGSF HIS mice suggests that ILC homeostasis may be regulated by similar Flt3L-dependent mechanisms, as found for human NK cells. We observed evidence for phenotypic diversity within the IFN-γ–producing ILCs in the liver of BRGSF mice, with TBET$^+$ cells heterogeneously expressing CD127 and CD94 that finds parallels with recent reports in humans.[19,44] Although the environmental factors that regulate human ILC1 diversity are not clearly identified, our BRGSF HIS mouse model provides a means to dissect ILC1 heterogeneity in tissue environments under steady-state and inflammatory conditions.

We identified functional GATA-3$^+$ human ILC2s in the lungs of BRGSF HIS mice. Previous studies have not yet described human ILC2s in humanized mice and, as such, the BRGSF model is unique in this regard. ILC2s play critical roles in immune protection against various pathogens (helminths, viruses) and are associated with atopic diseases and reactive airways (reviewed in Gladiator et al[11]). Moreover, ILC2s have been recently shown to have functional plasticity in the context of inflammation.[47,57,58] BRGSF HIS mice may provide a valuable new model to study the biology of human ILC2s in vivo in the context of inflammation.

We observed that BRGSF HIS mice support robust human immune reconstitution in the mouse intestine, including RORγt$^+$ ILC3. ILC3s play an important role in maintaining barrier function (reviewed in Montaldo et al[59]). Human intestinal ILC3s protect against colitis through production of IL-22 and regulate T cells by major histocompatibility complex class II–mediated presentation of microbial antigens,[60] a process that may be modeled in humanized mice.[61] Our BRGSF HIS mouse model may provide a means to dissect the biology of human intestinal immune

Figure 7. ILC3 can be found in the gut of BRGSF-reconstituted mice and their frequency increase after Flt3L treatment. (A) Total human CD45 cell number in gut of BRGSF mice treated or not with Flt3L. Composite data from of 12 to 16 mice per group. (B) Representative flow cytometry analysis of ILCs (CD3$^-$CD5$^-$CD94$^-$CD7$^+$CD127$^+$) in gut of reconstituted BRGSF mice treated or not with Flt3L. (C) Frequency among hCD45$^+$ cells and total number of ILCs in total gut of reconstituted BRGSF treated or not with Flt3L. Composite data from 6/8 mice of 2 experiments is shown. Each dot represents 1 mouse. (D) ILC (CD3$^-$CD5$^-$CD94$^-$CD7$^+$CD127$^+$) (red) expression of CD117 and NKp46 as compared with NK cells (gray). (E) Intracellular expression of RORγt in gut ILCs of a representative Flt3L-treated mouse and the corresponding quantification (top) and representative functional analysis by IL-22 and IL-17 intracellular flow cytometry from ex vivo–stimulated ILCs. (F) Quantification of IL-22 and IL-17 production analyzed by flow cytometry from CD3$^-$CD5$^-$CD94$^-$CD7$^+$CD127$^+$ ILC3 cells in response to TLR-mediated in vivo stimulation. Composite data from of 3 to 4 mice per condition are shown. Numbers in plots represent frequencies within gates.

tolerance. A recent report showed that HIV-1 infection depletes human ILC3, thus providing a plausible mechanism for loss of intestinal homeostasis in the context of this disease.[20] Enhanced human ILC3 development in BRGSF HIS mice offers a means to study these cells in various viral inflammation conditions.

Acknowledgments

This work was funded by the People Programme (Marie Curie Actions) of the European Union's Seventh Framework Programme FP7-PEOPLE-2012-ITN (The Natural Killer Cell-Based Anti-Cancer Immunotherapies project) under Research Executive Agency grant agreement no. 317013.

Authorship

Contribution: S.L.-L., G.M.-R., O.F., S.D., N.S., M.D., H.S.-M., and Y.L. performed experiments. S.L.-L. and J.P.D. designed research and wrote the manuscript.

Conflict-of-interest disclosure: J.P.D. is a stakeholder in AXENIS (founder, member of the executive board). The remaining authors declare no conflict of interest.

ORCID profiles: J.P.D., 0000-0002-7146-1862.

Correspondence to: James P. Di Santo, Innate Immunity Unit, INSERM U1223, Institut Pasteur, 25 rue du Docteur Roux, 75724 Paris, France; e-mail: james.di-santo@pasteur.fr.

References

1. Akkina R. New generation humanized mice for virus research: comparative aspects and future prospects. *Virology*. 2013;435(1):14-28.
2. Rongvaux A, Takizawa H, Strowig T, et al. Human hemato-lymphoid system mice: current use and future potential for medicine. *Annu Rev Immunol*. 2013; 31:635-674.
3. Theocharides APA, Rongvaux A, Fritsch K, Flavell RA, Manz MG. Humanized hemato-lymphoid system mice. *Haematologica*. 2016;101(1):5-19.
4. Serafini N, Vosshenrich CAJ, Di Santo JP. Transcriptional regulation of innate lymphoid cell fate. *Nat Rev Immunol*. 2015;15(7):415-428.
5. Spits H, Artis D, Colonna M, et al. Innate lymphoid cells—a proposal for uniform nomenclature. *Nat Rev Immunol*. 2013;13(2):145-149.
6. Herberman RB, Nunn ME, Lavrin DH. Natural cytotoxic reactivity of mouse lymphoid cells against syngeneic acid allogeneic tumors. I. Distribution of reactivity and specificity. *Int J Cancer*. 1975;16(2):216-229.
7. Cerwenka A, Lanier LL. Natural killer cells, viruses and cancer. *Nat Rev Immunol*. 2001;1(1):41-49.
8. Bernink JH, Krabbendam L, Germar K, et al. Interleukin-12 and -23 control plasticity of CD127(+) group 1 and group 3 innate lymphoid cells in the intestinal lamina propria. *Immunity*. 2015;43(1):146-160.
9. Spits H, Cupedo T. Innate lymphoid cells: emerging insights in development, lineage relationships, and function. *Annu Rev Immunol*. 2012;30(1): 647-675.
10. Hoyler T, Klose CSN, Souabni A, et al. The transcription factor GATA-3 controls cell fate and maintenance of type 2 innate lymphoid cells. *Immunity*. 2012;37(4):634-648.
11. Mjösberg J, Spits H. Type 2 innate lymphoid cells-new members of the "type 2 franchise" that mediate allergic airway inflammation. *Eur J Immunol*. 2012; 42(5):1093-1096.
12. Gladiator A, Wangler N, Trautwein-Weidner K, LeibundGut-Landmann S. Cutting edge: IL-17-secreting innate lymphoid cells are essential for host defense against fungal infection. *J Immunol*. 2013;190(2):521-525.
13. Gonçalves P, Di Santo JP. An intestinal inflammasome - the ILC3-cytokine tango. *Trends Mol Med*. 2016;22(4):269-271.
14. Takayama T, Kamada N, Chinen H, et al. Imbalance of NKp44(+)NKp46(-) and NKp44(-)NKp46(+) natural killer cells in the intestinal mucosa of patients with Crohn's disease. *Gastroenterology*. 2010;139(3):882-892, 892.e1-892.e3.
15. Legrand N, Huntington ND, Nagasawa M, et al. Functional CD47/signal regulatory protein alpha (SIRP(alpha)) interaction is required for optimal human T- and natural killer- (NK) cell homeostasis in vivo. *Proc Natl Acad Sci USA*. 2011;108(32):13224-13229.
16. Huntington ND, Legrand N, Alves NL, et al. IL-15 trans-presentation promotes human NK cell development and differentiation in vivo. *J Exp Med*. 2009; 206(1):25-34.
17. Strowig T, Chijioke O, Carrega P, et al. Human NK cells of mice with reconstituted human immune system components require preactivation to acquire functional competence. *Blood*. 2010;116(20):4158-4167.
18. Rongvaux A, Willinger T, Martinek J, et al. Development and function of human innate immune cells in a humanized mouse model. *Nat Biotechnol*. 2014; 32(4):364-372.
19. Bernink JH, Peters CP, Munneke M, et al. Human type 1 innate lymphoid cells accumulate in inflamed mucosal tissues. *Nat Immunol*. 2013;14(3): 221-229.
20. Zhang Z, Cheng L, Zhao J, et al. Plasmacytoid dendritic cells promote HIV-1-induced group 3 innate lymphoid cell depletion. *J Clin Invest*. 2015;125(9): 3692-3703.
21. Ito R, Takahashi T, Katano I, Ito M. Current advances in humanized mouse models. *Cell Mol Immunol*. 2012;9(3):208-214.
22. Shaw SG, Maung AA, Steptoe RJ, Thomson AW, Vujanovic NL. Expansion of functional NK cells in multiple tissue compartments of mice treated with Flt3-ligand: implications for anti-cancer and anti-viral therapy. *J Immunol*. 1998;161(6):2817-2824.
23. McKenna HJ, Stocking KL, Miller RE, et al. Mice lacking flt3 ligand have deficient hematopoiesis affecting hematopoietic progenitor cells, dendritic cells, and natural killer cells. *Blood*. 2000;95(11):3489-3497.

24. Guimond M, Freud AG, Mao HC, et al. In vivo role of Flt3 ligand and dendritic cells in NK cell homeostasis. *J Immunol*. 2010;184(6):2769-2775.

25. Baerenwaldt A, von Burg N, Kreuzaler M, et al. Flt3 ligand regulates the development of innate lymphoid cells in fetal and adult mice. *J Immunol*. 2016; 196(6):2561-2571.

26. Li Y, Mention J-J, Court N, et al. A novel Flt3-deficient HIS mouse model with selective enhancement of human DC development. *Eur J Immunol*. 2016; 46(5):1291-1299.

27. Chen Q, Khoury M, Chen J. Expression of human cytokines dramatically improves reconstitution of specific human-blood lineage cells in humanized mice. *Proc Natl Acad Sci USA*. 2009;106(51):21783-21788.

28. Maraskovsky E, Brasel K, Teepe M, et al. Dramatic increase in the numbers of functionally mature dendritic cells in Flt3 ligand-treated mice: multiple dendritic cell subpopulations identified. *J Exp Med*. 1996;184(5):1953-1962.

29. Shurin MR, Pandharipande PP, Zorina TD, et al. FLT3 ligand induces the generation of functionally active dendritic cells in mice. *Cell Immunol*. 1997; 179(2):174-184.

30. Pulendran B, Lingappa J, Kennedy MK, et al. Developmental pathways of dendritic cells in vivo: distinct function, phenotype, and localization of dendritic cell subsets in FLT3 ligand-treated mice. *J Immunol*. 1997;159(5):2222-2231.

31. Ding Y, Wilkinson A, Idris A, et al. FLT3-ligand treatment of humanized mice results in the generation of large numbers of CD141+ and CD1c+ dendritic cells in vivo. *J Immunol*. 2014;192(4):1982-1989.

32. Shah AJ, Smogorzewska EM, Hannum C, Crooks GM. Flt3 ligand induces proliferation of quiescent human bone marrow CD34+CD38- cells and maintains progenitor cells in vitro. *Blood*. 1996;87(9):3563-3570.

33. Kikushige Y, Yoshimoto G, Miyamoto T, et al. Human Flt3 is expressed at the hematopoietic stem cell and the granulocyte/macrophage progenitor stages to maintain cell survival. *J Immunol*. 2008;180(11):7358-7367.

34. Breton G, Lee J, Zhou YJ, et al. Circulating precursors of human CD1c+ and CD141+ dendritic cells. *J Exp Med*. 2015;212(3):401-413.

35. Lee J, Breton G, Oliveira TYK, et al. Restricted dendritic cell and monocyte progenitors in human cord blood and bone marrow. *J Exp Med*. 2015;212(3): 385-399.

36. Cooper MA, Fehniger TA, Caligiuri MA. The biology of human natural killer-cell subsets. *Trends Immunol*. 2001;22(11):633-640.

37. Lucas M, Schachterle W, Oberle K, Aichele P, Diefenbach A. Dendritic cells prime natural killer cells by trans-presenting interleukin 15. *Immunity*. 2007; 26(4):503-517.

38. Long EO. Ready for prime time: NK cell priming by dendritic cells. *Immunity*. 2007;26(4):385-387.

39. Sivori S, Carlomagno S, Pesce S, Moretta A, Vitale M, Marcenaro E. TLR/NCR/KIR: which one to use and when? *Front Immunol*. 2014;5:105.

40. Eberl G, Di Santo JP, Vivier E. The brave new world of innate lymphoid cells. *Nat Immunol*. 2015;16(1):1-5.

41. Spits H, Bernink JH, Lanier L. NK cells and type 1 innate lymphoid cells: partners in host defense. *Nat Immunol*. 2016;17(7):758-764.

42. Peng H, Jiang X, Chen Y, et al. Liver-resident NK cells confer adaptive immunity in skin-contact inflammation. *J Clin Invest*. 2013;123(4):1444-1456.

43. Peng H, Tian Z. Re-examining the origin and function of liver-resident NK cells. *Trends Immunol*. 2015;36(5):293-299.

44. Marquardt N, Béziat V, Nyström S, et al. Cutting edge: identification and characterization of human intrahepatic CD49a+ NK cells. *J Immunol*. 2015; 194(6):2467-2471.

45. Bernink JH, Germar K, Spits H. The role of ILC2 in pathology of type 2 inflammatory diseases. *Curr Opin Immunol*. 2014;31(31):115-120.

46. Mjösberg J, Spits H. Human innate lymphoid cells. *J Allergy Clin Immunol*. 2016;138(5):1265-1276.

47. Lim AI, Menegatti S, Bustamante J, et al. IL-12 drives functional plasticity of human group 2 innate lymphoid cells. *J Exp Med*. 2016;213(4): 569-583.

48. Mjösberg JM, Trifari S, Crellin NK, et al. Human IL-25- and IL-33-responsive type 2 innate lymphoid cells are defined by expression of CRTH2 and CD161. *Nat Immunol*. 2011;12(11):1055-1062.

49. Hoorweg K, Peters CP, Cornelissen F, et al. Functional differences between human NKp44(-) and NKp44(+) RORC(+) innate lymphoid cells. *Front Immunol*. 2012;3:72.

50. Crellin NK, Trifari S, Kaplan CD, Satoh-Takayama N, Di Santo JP, Spits H. Regulation of cytokine secretion in human CD127(+) LTi-like innate lymphoid cells by Toll-like receptor 2. *Immunity*. 2010;33(5):752-764.

51. de Saint-Vis B, Fugier-Vivier I, Massacrier C, et al. The cytokine profile expressed by human dendritic cells is dependent on cell subtype and mode of activation. *J Immunol*. 1998;160(4):1666-1676.

52. Scoville SD, Mundy-Bosse BL, Zhang MH, et al. A progenitor cell expressing transcription factor RORγt generates all human innate lymphoid cell subsets. *Immunity*. 2016;44(5):1140-1150.

53. Montaldo E, Teixeira-Alves LG, Glatzer T, et al. Human RORγt(+)CD34(+) cells are lineage-specified progenitors of group 3 RORγt(+) innate lymphoid cells. *Immunity*. 2014;41(6):988-1000.

54. Renoux VM, Zriwil A, Peitzsch C, et al. Identification of a human natural killer cell lineage-restricted progenitor in fetal and adult tissues. *Immunity*. 2015; 43(2):394-407.

55. van Beek JJP, Wimmers F, Hato SV, de Vries IJ, Sköld AE. Dendritic cell cross talk with innate and innate-like effector cells in antitumor immunity: implications for DC vaccination. *Crit Rev Immunol*. 2014;34(6):517-536.

56. Bouwer AL, Saunderson SC, Caldwell FJ, et al. NK cells are required for dendritic cell-based immunotherapy at the time of tumor challenge. *J Immunol*. 2014;192(5):2514-2521.

57. Silver JS, Kearley J, Copenhaver AM, et al. Inflammatory triggers associated with exacerbations of COPD orchestrate plasticity of group 2 innate lymphoid cells in the lungs. *Nat Immunol*. 2016;17(6):626-635.

58. Bal SM, Bernink JH, Nagasawa M, et al. IL-1β, IL-4 and IL-12 control the fate of group 2 innate lymphoid cells in human airway inflammation in the lungs. *Nat Immunol*. 2016;17(6):636-645.

59. Montaldo E, Juelke K, Romagnani C. Group 3 innate lymphoid cells (ILC3s): origin, differentiation, and plasticity in humans and mice. *Eur J Immunol*. 2015;45(8):2171-2182.

60. Hepworth MR, Monticelli LA, Fung TC, et al. Innate lymphoid cells regulate CD4+ T-cell responses to intestinal commensal bacteria. *Nature*. 2013; 498(7452):113-117.

61. Goettel JA, Gandhi R, Kenison JE, et al. AHR activation is protective against colitis driven by T cells in humanized mice. *Cell Reports*. 2016;17(5): 1318-1329.